Protective Role of Nrf2 in Zinc Oxide Nanoparticles-Induced Lung Inflammation in Female Mice and Sexual Dimorphism in Susceptibility

Radwa Sehsah
Mansoura University Faculty of Medicine
Wenting Wu
Nagoya University Graduate School of Medicine Faculty of Medicine: Nagoya Daigaku Daigakuin Igakukei Kenkyuka Igakubu
Sahoko Ichihara
Jichi Medical University: Jichi Ika Daigaku
Naozumi Hashimoto
Nagoya University: Nagoya Daigaku
Cai Zong
Tokyo University of Science: Tokyo Rika Daigaku
Kyoka Yamazaki
Tokyo University of Science: Tokyo Rika Daigaku
Harue Sato
Tokyo University of Science: Tokyo Rika Daigaku
Ken Itoh
Hirosaki University: Hirosaki Daigaku
Masayuki Yamamoto
Tohoku University: Tohoku Daigaku
Ahmed Ali Elsayed
Mansoura University
Soheir El-Bestar
Mansoura University
Emily Kamel
Mansoura University
Gaku Ichihara (gak@rs.tus.ac.jp)
Tokyo University of Science https://orcid.org/0000-0001-5707-5300

Research

Keywords: zinc oxide, nanoparticles, Nrf2, proinflammatory cytokines, sexual dimorphism

Posted Date: January 6th, 2022

DOI: https://doi.org/10.21203/rs.3.rs-1215458/v1

Abstract

Background

Zinc oxide nanoparticles (ZnO-NPs) are used in various products such as rubber, paint, and cosmetics. Our group reported recently that Nrf2 protein provides protection against ZnO-NPs-induced pulmonary inflammation in male mice. The present study investigated the effect of *Nrf2* deletion on the lung inflammatory response in female mice exposed to ZnO-NPs.

Methods

Twenty-four female $Nrf2^{-/-}$ mice and the same number of female $Nrf2^{+/+}$ mice were each divided into three equal groups and each exposed to ZnO-NPs at either 0, 10 or 30 μg/mouse by pharyngeal aspiration. Bronchoalveolar lavage fluid (BALF) and lungs were collected 14 days later to quantify protein level, number of inflammatory cells, and for scoring inflammation histopathologically. The mRNA levels of *Nrf2*-depedent antioxidant enzymes and proinflammatory cytokine in lung tissue were measured.

Results

Exposure to ZnO-NPs increased all types of BALF cells and lung inflammation scores in both of female $Nrf2^{-/-}$ and $Nrf2^{+/+}$ mice, and Nrf2 deletion enhanced ZnO-NPs-induced increase in the number of eosinophils in BALF. Nrf2 deletion enhanced ZnO-NPs-induced downregulation of *GR* and upregulation of *HO-1* and *TNFa.* Nrf2 deletion decreased mRNA levels of *CAT, GcLc* and *NQO1* and increased that for *GcLm* and *MT-2*. ZnO-NPs dose-dependently increased the level of oxidized glutathione (GSSG), and mRNA levels of proinflammatory cytokines/chemokines; *KC, MIP-2, IL-6, IL-1β* and *MCP-1* only in wild-type mice, and Nrf2 deletion decreased total glutathione levels and upregulated the above proinflammatory cytokines/chemokines regardless of level of exposure to ZnO-NPs. Taken together with our previous results in male mice, our results showed a lower susceptibility of females to lung inflammation, relative to males, irrespective of Nrf2 deletion, and that enhancement of ZnO-NPs-induced upregulation of *HO-1* and *TNFa* and downregulation of *GR* by deletion of Nrf2 is specific to female mice.

Conclusion

We conclude that Nrf2 provides protection in female mice against increase in BALF eosinophils, probably through down-regulation of proinflammatory cytokines/chemokines and upregulation of oxidative stress-related genes. The study also suggests lower susceptibility to lung inflammation in female mice relative to their male counterparts and the synergistic effects of sex and exposure to ZnO-NPs on mRNA expression of *GR, HO-1* or *TNFa.*

1 Introduction

During the last few years, zinc oxide nanoparticles (ZnO-NPs), among other metal oxide nanoparticles, have gained considerable attention. Their exceptional electronic, optical, mechanical, catalytic, magnetic, and chemical properties are the reason for their extensive use in several industrial applications and consumer products. They are, for example, used at present in cosmetics, sunscreens, textile, rubber, ceramics, paints, chemicals, solar cells, and electronics industries [1, 2]. Moreover, ZnO-NPs have significant potentials to pervade the biomedical field. They are also used in food packaging and ointments because of their anti-inflammatory, antimicrobial, and antifungal properties. They can also be potentially used in the future in biosensors, bioimaging, and drug and gene delivery [3–5]. With expanding applications of ZnO-NPs, increased exposure of humans is expected under various environmental and occupational settings. Occupational exposure can occur through inhalation or dermal routes, while consumers can be exposed through accidental dermal contact or ingestion, or intentionally through various biomedical applications. With the increased exposure to ZnO-NPs, concerns about their safety and potential toxicity for humans and animals have also been raised, making ZnO-NPs the focus of numerous investigative studies [6, 7]. In fact, several groups have examined the possible health effects of exposure to ZnO-NPs both *in vitro* and *in vivo* through different exposure routes. While some studies have described the beneficial effects of ZnO-NPs, others have highlighted their toxic effects on different cells and organ systems. Exposure to ZnO-NPs can induce mild but sometimes severe cytotoxicity, inflammation, genotoxicity, mutagenicity, neurotoxicity, pulmonary toxicity, cardiac toxicity,

hepatotoxicity, nephrotoxicity, intestinal toxicity, and reproductive toxicity [3, 7–9]. On the other hand, several other studies have focused on the mechanism(s) of ZnO-NPs-induced toxicities and different molecular mechanisms have been proposed. Among them, the generation of reactive oxygen species (ROS) and oxidative stress state, either directly by ZnO-NPs themselves or secondarily through toxic Zn^{+} ions generated from their dissolution, is considered the main mechanism of ZnO-NPs-induced toxicities. The proposed oxidative stress state initiates several deleterious cellular cascades and signaling pathways involved in the resultant toxicity, including the nuclear factor erythroid 2-related factor 2/antioxidant responsive element (Nrf2/ARE) pathway, which is one of the key endogenous antioxidant stress-protective pathway [3, 5, 8, 10–13].

The well-documented sex differences in anatomy and physiology can modify the responses to exogenous agents, and susceptibility, pathophysiology, incidence, course, morbidity, and mortality of several diseases across the lifetime and this is highly apparent in the epidemiology of lung diseases [14, 15]. Sex was found to be a key susceptibility candidate to engineered nanomaterials (ENMs)-induced lung inflammation, and with the expected occupational exposure to the nanoparticles primarily through inhalation, sex-related differences in the pulmonary responses to engineered nanomaterials have been the focus of attention recently [16].

The nuclear factor erythroid 2-related factor 2 (Nrf2) is a transcription factor involved in the regulation of various cell processes, including the regulation of the adaptive response and resistance to oxidant stress [17]. Our group reported recently that Nrf2 plays an important role in protection against ZnO-NPs-induced pulmonary cytotoxicity through the prevention of neutrophil migration in male mice [18]. However, it is still unknown whether Nrf2 has the same beneficial effects in female mice. The aim of the present study was to determine the effects of Nrf2 deletion on the ZnO-NPs-related pulmonary inflammatory response in female mice.

2 Materials And Methods

2.1 Zinc oxide nanoparticles. ZnO-NPs (MKN-ZnO-020) with primary diameter of 20 nm were purchased from mkNano (Mississauga, ONT, Canada). The surface area was measured by Brunauer-Emmett-Teller (BET) (Macsorb HM model-1201, MOUNTECH, Tokyo, Japan). Endotoxin analysis was conducted using Pierce LAL Chromogenic Endotoxin Quantification Kit (Thermo Scientific, Waltham, MA). A biocompatible dispersion medium (DM) was used to disperse the nanoparticles, which was Ca^{2+}- and Mg^{2+}-free phosphate buffered saline (PBS, pH 7.4), supplemented with 5.5 mM D-glucose, 0.6 mg/ml mouse serum albumin, and 0.01 mg/ml 1, 2-dipalmitoyl-sn-glycero-3-phosphocholine (DPPC) [19, 20]. The nanoparticles were dispersed in the DM to prepare a suspension with a concentration of 0.25 μg NP/ml DM for the low-dose group (10 μg/mouse), another with a concentration of 0.75 NP μg/ml DM for the high-dose group (30 μg/mouse), and a suspension with only DM, without nanoparticles, for the control group. The particles were dispersed using a cup-type sonicator (Branson Sonifier, cup horn), at 100 W, 80% pulse mode for 10 minutes. The hydrodynamic size was determined using dynamic light scattering (DLS) (Zetasizer Nano-S; Malvern Instruments, Worcestershire, UK).

2.2 Animals. *Nrf2*$^{-/-}$ female mice were generated as described by Itoh et al. [21] and backcrossed six times at the Central Institute for Experimental Animals (Kanagawa, Japan) and then further backcrossed seven times at the Division of Experimental Animals, Nagoya University Graduate School of Medicine (Nagoya, Japan). The genotypes of mice were confirmed by PCR amplification of genomic DNA isolated from the tail. PCR amplification was carried out using three different primers, 5#-TGGACGGGACTATTGAAGGCTG-3# (Nrf2-sense for both genotypes), 3#-GCCGCCTTTTCAGTAGATGGAGG-5# (Nrf2-antisense for wild-type), and 5#-GCGGATTGACCGTAATGGGATAGG-3# (Nrf2-antisense for LacZ). Another 24 pathogen-free age-matched C57BL/6JJcl female mice (*Nrf2*$^{+/+}$) weighing 22-27 g were purchased from CLEA Japan Inc. (Tokyo). All mice were housed and acclimatized in a clean environment for 1 week before the start of exposure experiments. Food and water were provided *ad libitum*. The animal room was light- and temperature-controlled with a 12-h light-dark cycle (lights on at 9 am and off at 9 pm), room temperature of 23-25°C and relative humidity at 57-60%. One day before the start of the experiment, mice of the two genotype groups were weighed and divided at random into three exposure groups (n=8 each); the control (0 μg ZnO-NPs), low-dose (10 μg ZnO-NPs) and high-dose (30 μg ZnO-NPs) groups. The latter two selected exposure doses are equivalent to 0.5 or 1.5 mg/kg body weight. The lower concentration of 0.5 mg/kg is comparable to deposition of 0.48 mg/kg in adult human lung from inhalation to ZnO for one week at the threshold limit value of 2 mg/m^3 (time-weighted average), as proposed by the American Conference of Governmental Industrial Hygienists (ACGIH), based on the values of 500 mL air/breath, 12 breath/min, 40 h/week [22].

The guide of the Japan Government Laws concerning the protection and control of animals, and the guide of animal experimentation of Nagoya University School of Medicine were followed throughout the experiments. The experiment protocol was approved by Nagoya University Animal Experiment Committee.

2.3 Pharyngeal aspiration of ZnO-NPs. Pharyngeal or oropharyngeal aspiration is proved to be an effective convenient alternative to inhalation exposure for the hazard assessment of nanomaterials [23]. For this purpose, the mouse was first anesthetized by intraperitoneal injection of pentobarbital, then suspended with a rubber band anchored around the upper incisors and placed on its back on an inclined board. ZnO-NP suspensions were vortexed for 10 seconds first, then the tongue was gently extended outside the oral cavity using blunt forceps, and 40 µl aliquot of the selected concentration was pipetted into the back of the tongue, which was pulled for 1 minute after pipetting then released. With the tongue protruded, the mouse was unable to swallow, and the liquid trickled down slowly into the lungs. Following release of the tongue, the mouse was gently lifted off the board, placed on its left side, and monitored for recovery from anesthesia.

2.4 Bronchoalveolar lavage (BAL), total and differential cell counts. Fourteen days after exposure, the mice were euthanized by intraperitoneal injection of a lethal dose of pentobarbital. The trachea and lungs of each mouse were exposed and bronchoalveolar lavage was conducted. For this purpose, an 18-gauge needle was inserted into the trachea and both lungs were lavaged by 1 ml of 10% PBS (gentle instillation and aspiration). The instillation and aspiration of PBS was repeated 5 times, making a total volume of 5 ml. The amount of recovered bronchoalveolar lavage fluid (BALF) was measured and recorded. The average volume of the retrieved fluid was >90% of the instilled; the amounts and recovery rates were not different among the three exposure groups. The collected BALF was kept on ice until centrifuged at 1500 rpm for 5 minutes, and the supernatant was aliquoted into three tubes and kept at –80°C until further analysis. The cell pellets were re-suspended in 1 ml of ACK lysis buffer (for red blood cells lysis) and left for 5 minutes at room temperature. Then 10 ml of 10% PBS were added and the whole volume was re-centrifuged at 1500 rpm for 5 minutes. The supernatant was discarded, and the cell pellet was re-suspended in 1 ml 10% PBS and kept on ice for use to determine the total and differential cell counts. Total cell count was determined using a ChemoMetec Nucleocounter (Allerød, Denmark), while differential cell count was performed under optical microscope on slides prepared by cytospin and stained with May-Grunwald-Giemsa (Merck, Darmstadt, Germany). The BALF cell types included macrophages, neutrophils, lymphocytes and eosinophils. The relative differential counts were presented as percentages of total cells counted in 10 fields of each cytospin smear. The absolute differential count was calculated as the product of the number of the total cell count and the proportion of the relative differential count.

2.5 Measurement of total protein in BALF. Total protein in BALF was measured using a Bio-Rad protein assay kit according to the instructions provided by the manufacturer (Bio-Rad Laboratories, Hercules, CA) with bovine serum albumin (BSA) as a standard.

2.6 Histopathological examination of the lung. After completion of BAL, the lungs were removed, washed in saline and the right lung was immediately frozen for further analysis. The left lung was fixed in 4% formalin, dehydrated with graded alcohol concentrations, embedded in paraffin, cut into 3 µm-thick sections, placed on slides, stained with hematoxylin and eosin (H&E) and examined under optical microscope by a pathologist blinded to the exposure. These lung sections were used to determine the degree of lung inflammation. The degree of peribronchial and perivascular inflammation was evaluated on a subjective scale of 0-3, as described previously [24–27]. A score of 0 represented no detectable inflammation, while score of 1 represented occasional cuffing with inflammatory cells. For score 2, most bronchi or vessels were surrounded by a thin layer (1-5 cells thick) of inflammatory cells. For score 3, most bronchi or vessels were surrounded by a thick layer (>5 cells thick) of inflammatory cells. Total lung inflammation was defined as the average of the peribronchial and perivascular inflammation scores. Four lung sections per mouse were scored and the inflammation score was expressed as the average value. Tissue slides were examined under an optical microscope (model DM750, Leica Microsystem, Wetzlar, Germany) and images were captured with Leica Application Suite V3 software.

2.7 Quantification of total glutathione and oxidized glutathione. The frozen lung tissue samples were homogenized with 5 volumes (w/v) of cold 50mM MES buffer (pH 6.01) containing 1mM EDTA. The protein in each sample was denatured with equal volume of 0.1% metaphosphoric acid (Sigma-Aldrich) and mixed on a vortex mixer. The mixture was allowed to stand at room temperature for 5 min and then centrifuged at 2000 x g for 3 min. The supernatant (95 µl) was kept at -20ºC until used for determination of total glutathione and oxidized glutathione (GSSG). First, 90 µl of supernatant was treated with 4.5 µl of 4M triethanolamine (Sigma-Aldrich) solution and vortexed well before assay. For the analysis of total reduced form of glutathione (GSH), 30 µl TEAM-treated sample was diluted 20-fold with MES buffer (pH 6.0) containing 2mM EDTA. An aliquot (50 µl) of the diluted solution was treated with 150 µl freshly prepared assay cocktail and assayed at 405 nm with a microplate reader (Gen5™ & Gen5 Secure, BioTek® Instruments, Inc.). For GSSG determination, 30 µl of TEAM-treated sample was diluted 10 times with MES buffer before derivatization with 2-vinylpyridine., Two µl of 1M 2-vinylpyridine was added to 200 µl of diluted solution of every sample or GSSG standard in tube, and then the tubes were mixed on a vortex mixer and incubated for 1 h at room temperature. Total GSH and GSSG

concentrations were calculated from a standard curve using GSSG (Cayman; 703014) prepared according to the GSH assay kit (Cayman Chemical Company, Ann Arbor, MI; #703002), and normalized versus protein concentration. Total GSH and GSSG were expressed in micromoles of GSH (or GSSG) per milligram of protein.

2.8 Malondialdehyde assay. The malondialdehyde (MDA) assay (Life Science Specialties, LLC; NWK-MDA01) was performed according to the protocol supplied by the manufacturer. A 10% wt/vol homogenate was prepared from lung tissue in cold Assay Buffer (Phosphate buffer, pH 7.0 with EDTA). Absorbance was read at 532 nm using a PowerScan4 microplate reader (DS Pharma Medical Co., Japan) after reaction of the sample with thiobarbituric acid (TBA). Samples were analyzed in duplicate, and MDA level was expressed in micromoles of MDA per milligram of protein.

2.9 RNA isolation and real-time quantitative reverse transcription-polymerase chain reaction (RT-PCR). The mRNA expression level of Nrf2-dependent genes; superoxide dismutase 1 *(SOD1)*, catalase *(CAT)*, glutamate-cysteine ligase catalytic subunit *(GcLc)*, glutamate-cysteine ligase modifier subunit *(GcLm)*, NAD(P)H quinone oxidoreductase *(NQO1)*, heme-oxygenase 1 *(HO-1)* and glutathione reductase *(GR)*, and metal-binding protein genes; metallothioneins *(MT-1 and MT-2)*, which protect against oxidative stress, and proinflammatory cytokines; tumor necrosis factor alpha *(TNF-α)*, interferon gamma *(IFN-γ)*, transforming growth factor beta *(TGF-β)*, interleukin-6 (*IL-6*), interleukin-1beta *(IL-1β)*, monocyte chemotactic protein-1 *(MCP-1)*, chemokine (C-X-C motif) ligand 1 *(CXCL1, KC)* and chemokine (C-X-C motif) ligand 2 *(CXCL2, MIP-2)*, fibrosis-related gene: matrix metalloproteinase 2 *(MMP2)* were measured in lung tissues. About 15 mg of frozen lung tissue from each animal were homogenized and total RNA was extracted using ReliaPrep^{TM} RNA Tissue Miniprep System, treated with DNase (Promega, WI) and kept at -80ºC until used. The RNA concentration was determined with a Nanodrop-1000 3.5.1 (Thermo Fisher Scientific, Waltham, MA). The quality of isolated RNA was assessed by calculating the A260/A280 ratio to ensure values between 1.7 and 2.0. For complementary DNA (cDNA) synthesis, SuperScript III Reverse transcriptase kit (Life Technologies, Carlsbad, CA) was used. The collected cDNA was kept at -30ºC until quantified by quantitative real-time PCR using AriaMx Real-Time PCR System (Agilent Technologies, Inc., Santa Clara, CA) and THUNDERBIRD SYBR qPCR Mix (Toyobo Co., Osaka, Japan) for *KC, MIP-2, IL-6, IL-1β* and *MCP-1* or using Mx3005P QRCP System (Agilent Technologies, Waldbronn, Germany) and Universal ProbeLibrary System Assay (Roche Diagnostics) for the other genes. The mRNA expression levels were normalized to *β-actin* for each gene. The sequences of the primers used in this study are shown in Supplementary Material (Table S1).

2.10 Statistical analysis. Data were expressed as mean ± standard deviation. Differences between the control and exposure groups were examined using Dunnett`s multiple comparison method following one-way ANOVA or Steel multiple comparison method following Kruskal Wallis nonparametric test in each genotype. To test a trend with level of exposure to ZnO-NPs, simple regression analysis or simple ordinal logistic regression analysis on the exposure level of ZnO nanoparticles was applied in each genotype separately. Multiple regression analysis or multiple ordinal logistic regression analysis using dummy variables for genotype in full model was applied to examine effect of interaction between genotype and exposure level. When the interaction between genotype and exposure level was not significant, multiple regression analysis on exposure level and genotype in a non-interaction model was applied to test the effects of exposure level and genotype.

Statistical analysis was performed using the JMP software version 16 (SAS Institute, Cary, NC) and probability (p) value <0.05 was considered statistically significant.

3 Results

3.1 Changes in body and lung weight

There was no significant difference in body weight and lung weight between ZnO-NPs exposure groups and the control, both for female wild-type mice and female Nrf2-null mice. The percentage of lung weight to body weight (relative lung weight) was significantly different between the ZnO-NPs exposure groups and the control only in wild-type mice (p=0.043, ANOVA), but not in Nrf2-null mice. However, post-ANOVA Dunnett's multiple comparison test did not show significant difference between the exposure groups and the control. Simple regression analysis showed significant trend with ZnO-NPs exposure level in wild-type mice (Table 1). Multiple regression analysis showed no significant interaction between ZnO-NPs exposure level and Nrf2 deletion in body weight, lung weight and relative lung weight. However, multiple regression analysis without interaction showed a significant negative effect

for Nrf2 on body and lung weights, as well as a positive effect for ZnO-NPs exposure on absolute lung weight and relative lung weight.

Table 1
Body and lung weight of mice at 14 days after exposure to zinc oxide nanoparticles by pharyngeal aspiration.

	Genotype	Level of ZnO-NPs (μg)			Simple regression	Multiple regression		
		0	10	30	Parameter estimate for ZnO-NPs	Parameter estimate for interaction of ZnO-NPs and Nrf2 deletion	Parameter estimate for ZnO-NPs	Parameter estimate for Nrf2 deletion
Body weight (g)	*Nrf2*$^{+/+}$	21.8±0.8	22.0±0.6	21.4±0.8	-0.016 (p=0.19)	0.029 (p=0.38)	-0.0017 (p=0.91)	-1.2 (p=0.0041)
	Nrf2$^{-/-}$	20.8±1.8	19.9±1.8	21.0±1.8	0.013 (p=0.68)			
Lung weight (mg)	*Nrf2*$^{+/+}$	324±23	321±20	345±33	0.77 (p=0.078)	-0.027 (p=0.97)	0.76 (p=0.029)	-18 (p=0.031)
	Nrf2$^{-/-}$	306±36	301±34	326±29	0.75 (p=0.18)			
Lung to body weight ratio (x10^{-3})	*Nrf2*$^{+/+}$	14.8±0.9	14.6±0.9	16.1±1.7	0.048 (p=0.025)	-0.021 (p=0.42)	0.037 (p=0.0069)	-0.031(p=0.93)
	Nrf2$^{-/-}$	14.8±1.4	15.1±1.1	15.6±0.8	0.027 (p=0.14)			

Data are mean ± SD.

* $p<0.05$, compared to the corresponding genotype control by ANOVA followed by Dunnett's multiple comparison test.

3.2 Changes in BALF cell count and total protein

Aspiration of ZnO-NPs induced significant changes in the absolute numbers of total and individual inflammatory cells in both the wild-type and Nrf2-null mice (ANOVA), with the exception of eosinophils in Nrf2-null mice, with significant changes at 10 and 30 mg of ZnO-NPs exposure compared to the non-exposed control group. Exposure to ZnO-NPs dose-dependently increased total cells, macrophages, lymphocytes, neutrophils and eosinophils in BALF in both the wild-type and Nrf2-null mice (simple regression analysis and simple ordinal logistic regression analysis, Table 2). Multiple regression analysis or multiple ordinal regression analysis did not show significant interaction between ZnO-NPs exposure level and Nrf2 deletion, and the analysis without interaction showed significant harmful effect for ZnO-NPs exposure level on total cells and all types of cells in BALF, and significant harmful effect for Nrf2 deletion only on eosinophils in BALF. Further simple regression analysis showed that exposure to ZnO-NPs dose-dependently decreased total protein only in wild-type mice, and multiple regression analysis without interaction showed significant harmful effect for ZnO-NPs exposure level on total protein.

Table 2

BALF cell counts and protein levels in female mice at 14 days after exposure to zinc oxide nanoparticles by pharyngeal aspiration.

	Genotype	Level of ZnO-NPs (μg)			Simple regression / simple ordinal logistic regression	Multiple regression / multiple ordinal logistic regression		
		0	10	30	Parameter estimation for ZnO-NPs	Parameter estimation for interaction of ZnO-NP and Nrf2 deletion	Parameter estimate for ZnO-NPs	Parameter estimate for Nrf2 deletion
Total cells ($\times 10^4$)	*Nrf2*$^{+/+}$	4.1±1.1	6.8±0.9*	9.1±1.8*	0.16 (p<0.0001)	0.062 (p=0.23)	0.19 (p<0.0001)	0.99 (p=0.13)
	Nrf2$^{-/-}$	4.8±1.1	6.8±3.0	11.4±3.7*	0.22 (p<0.0001)			
Macrophages ($\times 10^4$)	*Nrf2*$^{+/+}$	4.0±1.1	6.6±0.8*	8.7±1.8*	0.15 (p<0.0001)	0.056 (p=0.24)	0.18 (p<0.0001)	0.87 (p=0.15)
	Nrf2$^{-/-}$	4.7±0.9	6.4±2.8	10.8±3.4*	0.21 (p<0.0001)			
Lymphocytes ($\times 10^3$)	*Nrf2*$^{+/+}$	0.7±0.9	2.6±1.5*	3.6±0.9*	0.08(p=0.0001)	-0.0060 (p=0.88)	0.087 (p<0.0001)	0.45 (p=0.36)
	Nrf2$^{-/-}$	1.1±1.3	3.3±3.0	3.9±1.5*	0.08 (p=0.027)			
Neutrophils ($\times 10^2$)	*Nrf2*$^{+/+}$	0	0.5±0.6	1.5±2.1*	0.050 (p=0.021)	0.0039 (p=0.93)	-0.088 (p=0.0005)	-0.84 (p=0.15)
	Nrf2$^{-/-}$	0.07±0.19	0.99±0.78	2.9±3.4*	0.10 (p=0.0067)			
Eosinophils ($\times 10^2$)	*Nrf2*$^{+/+}$	0.1±0.3	0.5±0.6	5.2±5.8*	0.17 (p=0.0038)	-0.022 (p=0.63)	-0.17 (p<0.0001)	-1.6 (p=0.0053)
	Nrf2$^{-/-}$	0.31±0.61	2.9±2.7	23±36	0.78 (p=0.031)			
Total protein ($\times 10^{-1}$mg/ml)	*Nrf2*$^{+/+}$	1.0±0.1	1.1±0.3	0.8±0.2	-0.0082 (p=0.025)	-0.00059 (p=0.93)	-0.0085 (p=0.013)	0.058 (p=0.49)
	Nrf2$^{-/-}$	1.0±0.5	1.1±0. 3	0.8±0.2	-0.0088 (p=0.14)			

Data are mean ± SD.

*p<0.05, compared to the corresponding genotype control (by ANOVA followed by Dunnett's multiple comparison test for the number of total cells, macrophages and lymphocytes, and total protein or Kruskal Wallis nonparametric test followed by Steel multiple comparison test for neutrophil and eosinophil counts). Simple regression analysis for each genotype and multiple regression analysis in a model with interaction were conducted for the number of total cells, macrophages and lymphocytes, and total protein. Simple ordinal logistic regression analysis for each genotype and multiple ordinal logistic regression analysis in a model with interaction were conducted for neutrophil and eosinophil counts. Since the interaction was statistically insignificant for all of the examined parameters, multiple regression analysis or multiple ordinal logistic regression analysis was conducted in a model without interaction to estimate the separate effects of ZnO-NPs and Nrf2 deletion.

3.3 Changes in total inflammation score, peribronchial inflammation score and perivascular inflammation score

Exposure to ZnO-NPs increased significantly all of the examined scores at 30mg in both the wild-type mice and Nrf2-null mice (Kruskal Wallis nonparametric test followed by Steel multiple comparison test), and simple ordinal logistic regression analysis confirmed the significant trend with ZnO-NPs exposure level in both the wild-type and Nrf2-null mice (Table 3). Multiple ordinal logistic regression analysis with the full model did not show significant interactions between ZnO-NPs exposure level and Nrf2

deletion for all of the examined scores. Multiple ordinal logistic regression analysis without interaction showed significant effects of ZnO-NPs exposure level but no significant effect of Nrf2 deletion for all of the examined scores.

Table 3
Total inflammation score, perivascular inflammation score and peri-bronchial inflammation score in mice at 14 days after exposure to zinc oxide nanoparticles by pharyngeal aspiration

		Level of ZnO-NPs (μg)			Simple ordinal logistic regression	Multiple ordinal logistic regression		
	Genotype	0	10	30	Parameter estimate for ZnO-NPs	Parameter estimate for interaction of ZnO-NPs and Nrf2 deletion	Parameter estimate for ZnO-NPs	Parameter estimate for Nrf2 deletion
Total inflammation score	*Nrf2*$^{+/+}$	0±0	0.2±0.4	1.8±0.8*	0.35 (p=0.0020)	-0.066 (p=0.34)	-0.26 (p<0.0001)	-1.1 (p=0.15)
	Nrf2$^{-/-}$	0.06±0.18	0.06±0.18	2.4±0.5*	0.22 (p=0.0012)			
Peribronchial inflammation score	*Nrf2*$^{+/+}$	0±0	0.1±0.4	2.1±1.0*	0.35 (p=0.0036)	-0.083 (p=0.36)	-0.31 (p<0.0001)	-1.2 (p=0.18)
	Nrf2$^{-/-}$	0±0	0.1±0.4	2.8±0.5*	0.39 (p=0.0036)			
Perivascular inflammation score	*Nrf2*$^{+/+}$	0±0	0.3±0.5	1.4±0.7*	0.27 (p=0.0047)	-0.099 (p=0.20)	-0.22 (p<0.0001)	-0.94 (p=0.24)
	Nrf2$^{-/-}$	0.13±0.35	0±0	2.1±0.6*	0.21 (p=0.0027)			

Data are mean ± SD.

*p< 0.05, compared to the corresponding genotype control by Kruskal Wallis nonparametric test followed by Steel multiple comparison test. Simple ordinal logistic regression analysis for each genotype and multiple ordinal logistic regression analysis in a model with interaction were conducted. Since the interaction was statistically insignificant, multiple ordinal logistic regression analysis was conducted in a model without interaction to estimate the separate effects of ZnO-NPs and Nrf2 deletion.

3.4 Changes in glutathione and malondialdehyde expression levels in lung tissue

The GSSG/GSH ratio was significantly affected by the ZnO-NPs exposure level in wild-type mice (p=0.049, ANOVA), but the differences between the two exposed groups and the control were statistically insignificant (Dunnett's multiple comparison test). Simple regression analysis showed that ZnO-NPs exposure level had a significant effect on glutathione disulfide in wild-type mice (Table 4). No significant interactions between ZnO-NPs exposure level and Nrf2 deletion were noted in total glutathione, glutathione disulfide, GSSG/GSH rate and MDA (multiple regression analysis). On the other hand, Nrf2 deletion modulated significantly the levels of total glutathione, whereas ZnO-NPs exposure significantly altered glutathione disulfide expression level.

Table 4
Total glutathione (GSH), oxidized glutathione (GSSG), GSSG/total GSH ratio and malondialdehyde (MDA) in the lung of female mice at 14 days after exposure to zinc oxide nanoparticles by pharyngeal aspiration.

	Genotype	Level of ZnO-NPs (μg)			Simple regression	Multiple regression		
		0	10	30	Parameter estimate for ZnO-NPs	Parameter estimate for interaction of ZnO-NPs and Nrf2 deletion	Parameter estimate for ZnO-NPs	Parameter estimate for Nrf2 deletion
Total glutathione (nmol/g lung tissue)	*Nrf2*$^{+/+}$	63±16	57±12	67±8	0.21 (p=0.32)	-0.076 (p=0.78)	0.17 (p=0.20)	-23 (p<0.0001)
	Nrf2$^{-/-}$	39±11	37±11	43±8	0.13 (p=0.42)			
Glutathione disulfide (nmol/g lung tissue)	*Nrf2*$^{+/+}$	6.5±2.0	8.2±3.6	9.4±1.9	0.094 (p=0.037)	-0.047 (p=0.47)	0.070 (p=0.032)	-1.6 (p=0.053)
	Nrf2$^{-/-}$	5.5±2.9	6.9±3.5	7.1±2.5	0.047 (p=0.34)			
GSSG/GSH ratio (x10^{-1})	*Nrf2*$^{+/+}$	1.0±0.3	1.4±0.4	1.4±0.2	0.010 (p=0.071)	-0.0012 (p=0.92)	0.00095 (p=0.10)	0.029 (p=0.051)
	Nrf2$^{-/-}$	1.4±0.5	1.7±0.8	1.7±0.5	0.0089 (p=0.40)			
MDA (x10^{-1}nmol/mg protein)	*Nrf2*$^{+/+}$	2.7±1.9	2.2±0.4	1.8±0.4	-0.30 (p=0.11)	0.025 (p=0.19)	-0.018 (p=0.076)	-0.17 (p=0.48)
	Nrf2$^{-/-}$	2.1±0.7	2.1±0.2	2.0±0.2	-0.048 (p=0.48)			

Data are mean ± SD.

*p<0.05, compared to the corresponding genotype control (by ANOVA followed by Dunnett's multiple comparison test).

3.5 Changes in expression levels of lung oxidative stress-related genes (Table 5)

Table 5
mRNA levels of oxidative stress-related proteins relative to *β-actin*

	Genotype	Level of ZnO-NPs (μg)			Simple regression	Multiple regression		
		0	10	30	Effect of ZnO-NPs	Parameter estimate for interaction of ZnO-NPs and Nrf2 deletion	Parameter estimate for ZnO-NPs	Parameter estimate for Nrf2 deletion
SOD1	$Nrf2^{+/+}$	5.6±2.0	4.2±0.8	4.5±2.2	-0.029 (p=0.34)	0.037 (p=0.55)	-0.01 (p=0.74)	-0.66 (p=0.39)
	$Nrf2^{-/-}$	4.7±1.8	3.0±0.5	4.6±5.4	0.0082 (p=0.88)			
CAT	$Nrf2^{+/+}$	4.1±1.4	5.2±1.3	5.2±2.3	0.031 (p=0.28)	-0.044 (p=0.32)	0.0091 (p=0.68)	-1.5 (p=0.0071)
	$Nrf2^{-/-}$	4.1±2.1	2.4±0.7	3.4±2.4	-0.013 (p=0.70)			
GcLc	$Nrf2^{+/+}$	4.0±1.6	3.7±0.8	4.7±1.8	0.028 (p=0.25)	-0.051 (p=0.094)	0.0030 (p=0.84)	-2.0 (p<0.0001)
	$Nrf2^{-/-}$	2.8±1.0	1.8±0.6	1.9±1.2	-0.022 (p=0.20)			
GcLm	$Nrf2^{+/+}$	1.3±0.5	1.0±0.4	1.1±0.2	-0.0056 (p=0.37)	0.031 (p=0.077)	0.010 (p=0.26)	0.48 (p=0.036)
	$Nrf2^{-/-}$	1.4±0.9	1.4±0.5	2.1±1.4	0.026(p=0.13)			
NQO1	$Nrf2^{+/+}$	1.4±1.3	0.8±0.1	0.9±0.4	-0.015 (p=0.26)	0.017 (p=0.25)	-0.0069 (p=0.35)	-0.66 (p=0.0008)
	$Nrf2^{-/-}$	0.4±0.2	0.2±0.1	0.4±0.6	0.0016 (p=0.80)			
GR	$Nrf2^{+/+}$	24±10	21±10	20±6	-0.11 (p=0.44)	-0.39 (p=0.046)	-	-
	$Nrf2^{-/-}$	19±9	0.9±0.8*	1.5±1.7*	-0.50 (p=0.0008)			
HO-1	$Nrf2^{+/+}$	28±11.0	20±5	23±3	-0.14 (p=0.28)	1.8 (p=0.0037)	-	-
	$Nrf2^{-/-}$	18±8	68±25*	74±48*	1.6 (p=0.0084)			
MT-1	$Nrf2^{+/+}$	2.0±0.9	1.5±0.4	2.1±0.4	0.0062 (p=0.58)	-0.021 (p=0.68)	-0.0045 (p=0.86)	1.0 (p=0.12)
	$Nrf2^{-/-}$	3.4±3.2	2.5±3.1	2.8±3.1	-0.0015 (p=0.77)			

Data are mean ± SD.

* $p<0.05$, compared to the corresponding genotype control by ANOVA followed by Dunnett's multiple comparison test.

	Genotype	Level of ZnO-NPs (μg)			Simple regression	Multiple regression		
		0	10	30	Effect of ZnO-NPs	Parameter estimate for interaction of ZnO-NPs and Nrf2 deletion	Parameter estimate for ZnO-NPs	Parameter estimate for Nrf2 deletion
MT-2	*Nrf2*$^{+/+}$	2.6±1.7	1.5±0.4	2.4±0.8	-0.0011 (p=0.96)	-0.050 (p=0.51)	-0.026 (p=0.48)	2.0 (p=0.040)
	Nrf2$^{-/-}$	4.1±2.6	5.3±6.7	2.9±2.7	-0.051 (p=0.48)			

Data are mean ± SD.

* $p<0.05$, compared to the corresponding genotype control by ANOVA followed by Dunnett's multiple comparison test.

There were no significant ZnO-NPs dose-related differences in the gene expression levels in Nrf2-null mice with the exception of *GR* (p<0.0001, ANOVA) and *HO-1* (p=0.0036, ANOVA). Further analysis with the Dunnett's multiple comparison test showed that exposure to the two doses of ZnO-NPs was associated with significant decreases in *GR* and significant increases in *HO-1* in Nrf2-null mice. Furthermore, simple regression analyses confirmed the significant trends of *GR* and *HO-1* with exposure level (Table 5). Multiple regression analysis showed significant interaction of ZnO-NPs exposure level with *GR* and *HO-1*, but not with other genes. Nrf2 deletion was associated with significant overexpression of *GcLm* and *MT-2* and under-expression of *CAT*, *GcLc* and *NQO1*.

3.6 Changes in expression levels of lung proinflammatory cytokines and fibrosis-related proteins

At 30 μg exposure level, ZnO-NPs significantly increased the expression levels of *KC*, *MIP-2*, *IL-6, IL-1β, MCP-1* and *MMP2* (ANOVA followed by Dunnett's test) and these changes were confirmed by simple regression analysis in wild-type mice (Table 6). Multiple regression analysis showed no significant interaction of ZnO-NPs exposure level with Nrf2 deletion for all the tested cytokines and *MMP2*. Non-interaction multiple regression analysis showed ZnO-NPs exposure significantly altered the expression levels of *MMP2* whereas Nrf2 deletion significantly affected the levels of *KC, MIP-2, IL-6, IL-1β, MCP-1* and *TNFα.*

Table 6
mRNA levels of pro-inflammatory cytokines and fibrosis-related proteins relative to *β-actin.*

	Genotype	Level of ZnO-NPs (μg)			Simple regression	Multiple regression		
		0	10	30	Parameter estimate for ZnO-NPs	Parameter estimate for interaction of ZnO-NPs and Nrf2 deletion	Parameter estimate for ZnO-NPs	Parameter estimate for Nrf2 deletion
KC	$Nrf2^{+/+}$	0.4±0.3	0.4±0.3	1.2±0.7*	0.028 (p=0.0013)	-0.00033 (p=0.99)	0.028 (p=0.13)	1.5 (p=0.0016)
	$Nrf2^{-/-}$	2.1±1.8	1.6±1.0	2.8±3.1	0.028 (p=0.45)			
MIP-2	$Nrf2^{+/+}$	0.5±0.2	0.4±0.3	1.0±0.3*	0.017 (p=0.0031)	-0.033 (p=0.19)	0.00024 (p=0.98)	1.7 (p<0.0001)
	$Nrf2^{-/-}$	2.6±2.3	2.3±0.9	2.1±0.9	-0.016 (p=0.52)			
IL-6	$Nrf2^{+/+}$	0.4±0.1	0.4±0.2	1.3±05*	0.032 (p<0.0001)	-0.017 (p=0.64)	0.023 (p=0.19)	1.4 (p=0.0030)
	$Nrf2^{-/-}$	2.2±2.1	1.6±1.3	2.5±2.6	0.015 (p=0.67)			
IL-1β	$Nrf2^{+/+}$	0.15±0.06	0.24±0.15	0.50±0.24*	0.012 (p=0.0004)	-0.013 (p=0.23)	0.0050 (p=0.36)	0.59 (p<0.0001)
	$Nrf2^{-/-}$	1.0±0.9	0.74±0.46	0.91±0.51	-0.0014 (p=0.89)			
MCP-1	$Nrf2^{+/+}$	0.39±0.12	0.34±0.15	0.86±0.30*	0.017 (p=0.0002)	-0.023 (p=0.32)	0.0053 (p=0.65)	1.1 (p=0.0002)
	$Nrf2^{-/-}$	2.1±1.9	1.3±0.5	1.7±1.2	-0.06 (p=0.79)			
TGF-β	$Nrf2^{+/+}$	2.4±0.9	3.1±0.8	3.1±1.5	0.022 (p=0.24)	-0.037 (p=0.21)	0.0039 (p=0.79)	-0.54 (p=0.14)
	$Nrf2^{-/-}$	2.8±0.8	1.9±0.5	2.2±2.1	-0.015 (p=0.52)			
TNF-α	$Nrf2^{+/+}$	1.3±0.4	1.5±0.5	1.3±0.3	0.00017 (p=0.98)	0.13 (p=0.12)	0.065 (p=0.14)	3.7 (p=0.0012)
	$Nrf2^{-/-}$	1.4±0.6	7.1±5.2	6.5±6.4	0.13 (p=0.14)			
IFN-γ	$Nrf2^{+/+}$	2.5±1.7	1.9±0.6	1.9±1.0	-0.018 (p=0.38)	0.056 (p=0.29)	0.010 (p=0.70)	0.86 (p=0.20)
	$Nrf2^{-/-}$	2.7±3.2	2.5±0.9	3.7±3.9	0.038 (p=0.43)			
MMP2	$Nrf2^{+/+}$	1.1±0.6	1.0±0.3	1.7±0.4*	0.022 (p=0.0065)	0.029 (p=0.29)	0.037 (p=0.010)	0.35 (p=0.31)
	$Nrf2^{-/-}$	1.1±0.6	1.3±0.6	2.6±2.7	0.051 (p=0.064)			

Data are mean ± SD.

* $p<0.05$, compared to the corresponding genotype control by ANOVA followed by Dunnett's multiple comparison test.

4 Discussion

The present study showed that Nrf2 deletion additively enhanced the effects of exposure to ZnO-NPs on the number of eosinophils in BALF of female mice. This is accompanied by enhancement of ZnO-NPs-induced upregulation of *HO-1* and *TNFα* and ZnO-NPs-induced down-regulation of *GR* by Nrf2 deletion, in addition to reduction of total glutathione, downregulation of *CAT, GcLc* and *NQO1* mRNA levels and upregulation of *KC, MIP-2, IL-6, IL-1β* and *MCP-1* mRNA levels by Nrf2 deletion. The results indicated that in female mice, Nrf2 inhibits infiltration of eosinophils in the lung, at least in part through upregulation of anti-oxidative stress genes and downregulation of proinflammatory cytokines or chemokines.

Our results showed that Nrf2 deletion increased eosinophils in BALF of female mice in agreement with the results of male mice [18]. However, the results showed Nrf2 deletion only marginally increased total cells and macrophages in BALF of female mice without significant difference. This is different from the results of male mice, which showed that Nrf2 deletion significantly increased the number of total cells and macrophages in BALF [18], and the difference seems due to less magnitude of increase in macrophages in female Nrf2 null mice compared to male Nrf2 null mice. In line with less infiltration of macrophages in the lung of female Nrf2 null mice compared to male Nrf2 null mice, comparison of the lung inflammation score in our female mice with that of male mice [18] suggests weaker susceptibility of the female relative to the male regardless of Nrf2 deletion. This difference in sex-related susceptibility might be partially explained by higher basal expression of *HO-1* or *GR* in female mice than male mice regardless of Nrf2 deletion [18]. Relative expression levels of *HO-1* and *GR* in 0μg ZnO-NP group of female wild type mice were 28±11 and 24±10 respectively, while those of male wild type mice were 7.5±3.0 and 1.3±0.3 respectively [18]. Relative expression levels of *HO-1* and *GR* in 0μg ZnO-NP group of *HO-1* and *GR* in 0μg ZnO-NP group of female Nrf2 null mice were 18±8 and 19±9 respectively, while those of male Nrf2 null mice were 5.8±2.5 and 2.1±0.5 respectively [18]. A previous study showed that male mice were more susceptible to acute and chronic pulmonary inflammation following single and repeated exposure to nickel nanoparticles than female mice [28]. In contrast, Shvedova et al. reported more severe pulmonary toxicity in female mice exposed to cellulose nanocrystals compared to male mice [29]. Another study showed enhanced susceptibility of female mice to acute and chronic lung inflammation induced by multi-walled carbon nanotubes (MWCNTs) [30]. Further studies are needed to explain the above differences in the sex-related susceptibility to toxicity.

Nrf2 deletion enhanced ZnO-NPs-induced upregulation of *HO-1* and *TNFα* and downregulation of *GR* in female mice, but not in male mice [18]. It is known that *HO-1* and *GR* expression shows sexual dimorphisms and is regulated by estradiol [31–35]. Trauma and hemorrhage are reported to induce a 2-fold increase in hepatic *HO-1* expression in proestrus female rats compared to male rats [34]. Treatment with 17β-estradiol upregulate the expression of *HO-1* in the liver of mice [33]. The findings of another *in vivo* study suggested that increased HO activity and expression in female rats compared to male rats can explain the sexual dimorphism of cardiovascular ischemia during reproductive age [31]. Finally, higher activity of GR from 4 to 24 weeks of age was described in the liver of male rats compared to female rats [32]. The mechanism for the sexual dimorphism in expression of *HO-1* or *GR* remains elusive. In vitro studies have shown that 17β-estradiol can upregulate Nrf2 in nuclear extracts and increase the expression of *HO-1, SOD, GST* and *GCL* in hypoxia/reoxygenation model of primary myocardial cells [35] and 17β-estradiol increases Nrf2 activity through activation of the PI3K pathway in MCF-1 breast cancer cells [36]. However, these studies on Nrf2 activation by estradiol cannot explain our results that ZnO-NPs-induced upregulation of HO-1 is enhanced in Nrf2 null mice.

Although *HO-1* plays an adverse role in carcinogenesis and neurodegenerative disease, it is known to play a protective role against oxidative injury and other stress conditions [37]. We believe that ZnO-NPs-induced upregulation of *HO-1* in female mice only is involved with the observed low susceptibility of female mice to peribronchial inflammation compared to male mice, though further studies are needed to test this hypothesis.

Nrf2 deletion significantly increased eosinophil in BALF, while did not significantly increase the lung inflammation score in female mice. This is in agreement with the previous study on male Nrf2 null mice and wild type mice, suggesting limitation of semi-quantification in inflammation scoring [18].

In conclusion, our study demonstrated the protective role of Nrf2 against ZnO-NPs-induced infiltration of eosinophils in lung of female mice, which might be explained by negative regulation of proinflammatory cytokines and chemokines and positive regulation of oxidative stress-related genes by Nrf2. The results also suggested lower susceptibility to lung inflammation in female mice compared with male mice and the synergistic effect of sex and ZnO-NPs exposure on *GR, HO-1* or *TNFα* mRNA expression, although further studies are needed to define the relationship between sex-related susceptibility and gene expression.

Declarations

Ethics approval

The guide of Japanese law concerning protection and control of animals and the guide of animal experimentation of Nagoya University School of Medicine were followed throughout the experiments. The animal experiment protocol was approved by Nagoya University Animal Experiment Committee.

Consent for publication

All authors consent for publication

Availability of data and material

The authors declare that the data supporting the findings of this study are available within the paper.

Competing interests

All authors declare no competing interests with the present study.

Funding

This work was supported by Japan Society for the Promotion of Science [NEXT Program #LS056], a grant-in aid for Scientific Research (#26293149), and Japan Science and Technology Agency (JST) Strategic Japanese-EU Cooperative Program: study on managing the potential health and environmental risks of engineered nanomaterials.

Authors' contributions

R.S. and G.I planned the experiment and wrote the manuscript. R.S., W.W. S.I. and N.H. conducted the animal experiment. R.S., C.Z. K.Y and H.S. conducted analysis of quantitative real time PCR. K.I. and M.Y. prepared $Nrf2^{-/-}$ mice. A.A.E. evaluated histopathology of murine lung. S.E. and E.K. read the manuscript and gave constructive comments.

Acknowledgments

We thank Ms. Satoko Arai for the excellent secretarial support.

References

1. Kolodziejczak-Radzimska A and Jesionowski T:**Zinc Oxide-From Synthesis to Application: A Review.***Materials (Basel)* 2014, **7**: 2833-2881.
2. Parihar V, Raja M, and Paulose R:**A Brief Review of Structural, Electrical and Electrochemical Properties of Zinc Oxide Nanoparticles.***Reviews on Advanced Materials Science* 2018, **53**: 119-130.
3. Keerthana S and Kumar A:**Potential risks and benefits of zinc oxide nanoparticles: a systematic review.***Critical Reviews in Toxicology* 2020, **50**: 47-71.
4. Mishra PK, Mishra H, Ekielski A, Talegaonkar S, and Vaidya B:**Zinc oxide nanoparticles: a promising nanomaterial for biomedical applications.***Drug Discovery Today* 2017, **22**: 1825-1834.
5. Sruthi S, Ashtami J, and Mohanan PV:**Biomedical application and hidden toxicity of Zinc oxide nanoparticles.***Materials Today Chemistry* 2018, **10**: 175-186.
6. Liao CZ, Jin YM, Li YC, and Tjong SC:**Interactions of Zinc Oxide Nanostructures with Mammalian Cells: Cytotoxicity and Photocatalytic Toxicity.***International Journal of Molecular Sciences* 2020, **21**.
7. Sruthi S and Mohanan PV:**Engineered Zinc Oxide Nanoparticles; Biological Interactions at the Organ Level.***Current Medicinal Chemistry* 2016, **23**: 4057-4068.
8. Singh S:**Zinc oxide nanoparticles impacts: cytotoxicity, genotoxicity, developmental toxicity, and neurotoxicity.***Toxicology Mechanisms and Methods* 2019, **29**: 300-311.

9. Singh TA, Das J, and Sil PC:**Zinc oxide nanoparticles: A comprehensive review on its synthesis, anticancer and drug delivery applications as well as health risks.***Advances in Colloid and Interface Science* 2020, **286**.
10. Attarilar S, Yang JF, Ebrahimi M, Wang QG, Liu J, Tang YJ, and Yang JL:**The Toxicity Phenomenon and the Related Occurrence in Metal and Metal Oxide Nanoparticles: A Brief Review From the Biomedical Perspective.***Frontiers in Bioengineering and Biotechnology* 2020, **8**.
11. Li BJ and Tang M:**Research progress of nanoparticle toxicity signaling pathway.***Life Sciences* 2020, **263**.
12. Roy R, Das M, and Dwivedi PD:**Toxicological mode of action of ZnO nanoparticles: Impact on immune cells.***Molecular Immunology* 2015, **63**: 184-192.
13. Saptarshi SR, Duschl A, and Lopata AL:**Biological reactivity of zinc oxide nanoparticles with mammalian test systems: an overview.***Nanomedicine* 2015, **10**: 2075-2092.
14. Sathish V, Martin YN, and Prakash YS:**Sex steroid signaling: Implications for lung diseases.***Pharmacology & Therapeutics* 2015, **150**: 94-108.
15. Silveyra P, Fuentes N, and Bauza DER:**Sex and Gender Differences in Lung Disease.***Lung Inflammation in Health and Disease, Vol Ii* 2021, **1304**: 227-258.
16. You DJ and Bonner JC:**Susceptibility Factors in Chronic Lung Inflammatory Responses to Engineered Nanomaterials.***International Journal of Molecular Sciences* 2020, **21**.
17. Ma Q:**Role of Nrf2 in Oxidative Stress and Toxicity.***Annual Review of Pharmacology and Toxicology, Vol 53, 2013* 2013, **53**: 401-+.
18. Sehsah R, Wu WT, Ichihara S, Hashimoto N, Hasegawa Y, Zong C, Itoh K, Yamamoto M, Elsayed AA, El-Bestar S, Kamel E, and Ichihara G:**Role of Nrf2 in inflammatory response in lung of mice exposed to zinc oxide nanoparticles.***Particle and Fibre Toxicology* 2019, **16**.
19. Porter D, Sriram K, Wolfarth M, Jefferson A, Schwegler-Berry D, Andrew M, and Castranova V:**A biocompatible medium for nanoparticle dispersion.***Nanotoxicology* 2008, **2**: 144-154.
20. Wu WT, Ichihara G, Suzuki Y, Izuoka K, Oikawa-Tada S, Chang J, Sakai K, Miyazawa K, Porter D, Castranova V, Kawaguchi M, and Ichihara S:**Dispersion Method for Safety Research on Manufactured Nanomaterials.***Industrial Health* 2014, **52**: 54-65.
21. Itoh K, Chiba T, Takahashi S, Ishii T, Igarashi K, Katoh Y, Oyake T, Hayashi N, Satoh K, Hatayama I, Yamamoto M, and Nabeshima Y:**An Nrf2/small Maf heterodimer mediates the induction of phase II detoxifying enzyme genes through antioxidant response elements.***Biochem Biophys Res Commun* 1997, **236**: 313-22.
22. Scanlan CR, Wilkins RL, and Stoller JK, *Egan's Fundamental of Respiratory Care*. 7th ed. 1999, St. Louis, Missouri, USA: Mosby, Inc. 1238.
23. Kinaret P, Ilves M, Fortino V, Rydman E, Karisola P, Lahde A, Koivisto J, Jokiniemi J, Wolff H, Savolainen K, Greco D, and Alenius H:**Inhalation and Oropharyngeal Aspiration Exposure to Rod-Like Carbon Nanotubes Induce Similar Airway Inflammation and Biological Responses in Mouse Lungs.***ACS Nano* 2017, **11**: 291-303.
24. Braber S, Henricks PAJ, Nijkamp FP, Kraneveld AD, and Folkerts G:**Inflammatory changes in the airways of mice caused by cigarette smoke exposure are only partially reversed after smoking cessation.***Respiratory Research* 2010, **11**.
25. Kwak YG, Song CH, Yi HK, Hwang PH, Kim JS, Lee KS, and Lee YC:**Involvement of PTEN in airway hyperresponsiveness and inflammation in bronchial asthma.***Journal of Clinical Investigation* 2003, **111**: 1083-1092.
26. Braber S, Henricks PA, Nijkamp FP, Kraneveld AD, and Folkerts G:**Inflammatory changes in the airways of mice caused by cigarette smoke exposure are only partially reversed after smoking cessation.***Respir Res* 2010, **11**: 99.
27. Kwak YG, Song CH, Yi HK, Hwang PH, Kim JS, Lee KS, and Lee YC:**Involvement of PTEN in airway hyperresponsiveness and inflammation in bronchial asthma.***J Clin Invest* 2003, **111**: 1083-92.
28. You DJ, Lee HY, Taylor-Just AJ, Linder KE, and Bonner JC:**Sex differences in the acute and subchronic lung inflammatory responses of mice to nickel nanoparticles.***Nanotoxicology* 2020, **14**: 1058-1081.
29. Shvedova AA, Kisin ER, Yanamala N, Farcas MT, Menas AL, Williams A, Fournier PM, Reynolds JS, Gutkin DW, Star A, Reiner RS, Halappanavar S, and Kagan VE:**Gender differences in murine pulmonary responses elicited by cellulose nanocrystals.***Particle and Fibre Toxicology* 2016, **13**.

30. Ray JL and Holian A:**Sex differences in the inflammatory immune response to multi-walled carbon nanotubes and crystalline silica.***Inhalation Toxicology* 2019, **31**: 285-297.
31. Posa A, Kupai K, Menesi R, Szalai Z, Szabo R, Pinter Z, Palfi G, Gyongyosi M, Berko A, Pavo I, and Varga C:**Sexual Dimorphism of Cardiovascular Ischemia Susceptibility Is Mediated by Heme Oxygenase.***Oxidative Medicine and Cellular Longevity* 2013, **2013**.
32. Rikans LE, Moore DR, and Snowden CD:**Sex-Dependent Differences in the Effects of Aging on Antioxidant Defense-Mechanisms of Rat-Liver.***Biochimica Et Biophysica Acta* 1991, **1074**: 195-200.
33. Safranko ZM, Sobocanec S, Saric A, Jajcanin-Jozic N, Krsnik Z, Aralica G, Balog T, and Abramic M:**The effect of 17 beta-estradiol on the expression of dipeptidyl peptidase III and heme oxygenase 1 in liver of CBA/H mice.***Journal of Endocrinological Investigation* 2015, **38**: 471-479.
34. Toth B, Yokoyama Y, Kuebler JF, Schwacha MG, Rue LW, Bland KI, and Chaudry IH:**Sex differences in hepatic heme oxygenase expression and activity following trauma and hemorrhagic shock.***Archives of Surgery* 2003, **138**: 1375-1382.
35. Yu JJ, Zhao YL, Li BJ, Sun LL, and Huo HL:**17 beta-Estradiol regulates the expression of antioxidant enzymes in myocardial cells by increasing Nrf2 translocation.***Journal of Biochemical and Molecular Toxicology* 2012, **26**: 264-269.
36. Wu JJ, Williams D, Walter GA, Thompson WE, and Sidell N:**Estrogen increases Nrf2 activity through activation of the PI3K pathway in MCF-7 breast cancer cells.***Experimental Cell Research* 2014, **328**: 351-360.
37. Waza AA, Hamid Z, Ali S, Bhat SA, and Bhat MA:**A review on heme oxygenase-1 induction: is it a necessary evil.***Inflammation Research* 2018, **67**: 579-588.

Figures

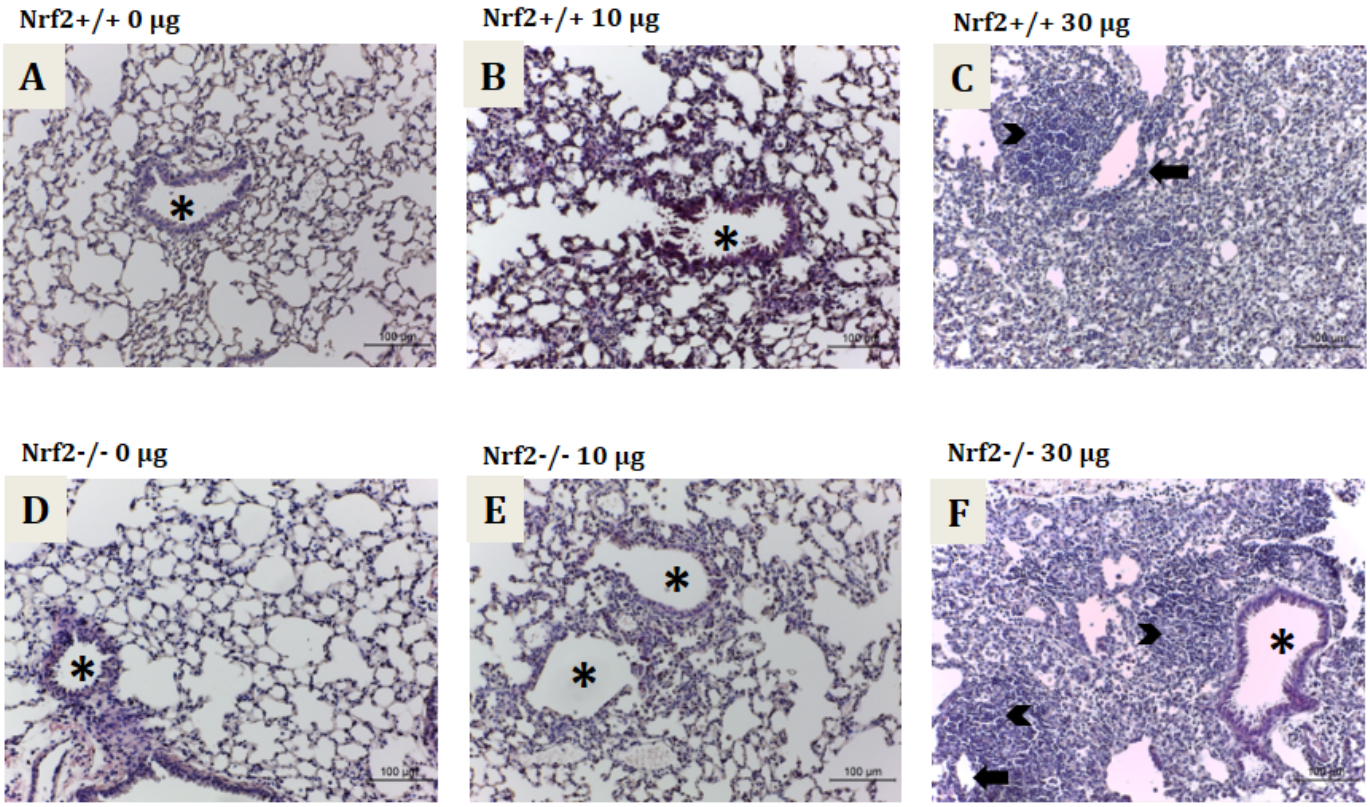

Figure 1

(**A**) *Nrf2*$^{+/+}$ no ZnO-NPs, no detectable inflammation in bronchioles (asterisk); (**B**) *Nrf2*$^{+/+}$ 10 µg ZnO-NPs. Note the presence of a thin layer (1-5 cells thick) of inflammatory cells surrounding the bronchioles (asterisk); (**C**) *Nrf2*$^{+/+}$ 30 µg ZnO-NPs. Note that the blood vessels (arrow) are surrounded by a thick layer of inflammatory cells (>5 cells thick) with lymphoid follicle formation (arrowhead);

(**D**) *Nrf2*$^{-/-}$ no ZnO-NPs. Notre the lack of detectable inflammation around bronchioles (asterisk); (**E**) *Nrf2*$^{-/-}$ 10 µg ZnO-NPs. Note the thin layer (1-5 cells thick) of inflammatory cells surrounding the bronchioles (asterisk); (**F**) *Nrf2*$^{-/-}$ 30 µg ZnO-NPs. Note the thick layer (>5 cells thick) of inflammatory cells surrounding the bronchioles (asterisk) and vessels (arrow), and formation of lymphoid follicles (arrowhead).

Supplementary Files

This is a list of supplementary files associated with this preprint. Click to download.

- RadwaFemaleSupplementaryTable1S.docx